Decoupling intranode and internode scattering in Weyl fermions

G. Sharma, Snehasish Nandy, Karthik V. Raman, and Sumanta Tewari ¹School of Basic Sciences, Indian Institute of Technology Mandi, Mandi 175005, India ²Department of Physics, University of Virginia, Charlottesville, Virginia 22904, USA ³Tata Institute of Fundamental Research, Hyderabad, Telangana 500046, India ⁴Department of Physics and Astronomy, Clemson University, Clemson, South Carolina 29634, USA



(Received 20 February 2022; revised 23 July 2022; accepted 16 March 2023; published 28 March 2023)

A series of recent papers claimed that intranode scattering alone can contribute to positive longitudinal magnetoconductance (LMC) due to the chiral anomaly (CA) in Weyl semimetals (WSMs) in the quasiclassical limit. We revisit the problem of CA-induced LMC in WSMs in the quasiclassical limit and show that intranode scattering, by itself, does not result in enhancement of LMC. In the limit of zero internode scattering, chiral charge must remain conserved, which is shown to actually decrease LMC. Only in the presence of a finite nonzero internode scattering does one obtain a positive LMC due to nonconservation of the chiral charge. Even weak internode scattering suffices in generating positive LMC since it redistributes charges across both the nodes, although on a timescale larger than that of the intranode scattering. Our work is fundamental to correctly interpret the recent experiments on magnetoconductance in Weyl semimetals that claim to have observed chiral anomaly. Furthermore, our calculations reveal that, in contrast to recent works, in inhomogeneous WSMs strain-induced axial magnetic field B₅, by itself, leads to negative longitudinal magnetoconductance and a negative planar Hall conductance.

DOI: 10.1103/PhysRevB.107.115161

I. INTRODUCTION

Chiral anomaly (CA) finds its genesis in high-energy physics [1,2], whereby the left/right-handed Weyl fermions are not conserved in the presence of nonorthogonal electric and magnetic fields. The anomaly has resurged in Weyl semimetals (WSMs) and has been of great interest in the condensed-matter community over the last decade [3–30]. Since Weyl semimetals host Weyl fermions as quasiparticle excitations, chiral anomaly is expected to occur in these materials in the presence of external electromagnetic fields. Positive longitudinal magnetoconductance (LMC) [10] and the planar Hall effect (PHE) [31] are some key signatures to identify the manifestation of chiral anomaly in Weyl semimetals. Some nonelectronic probes of chiral anomaly include optical processes as well [32–38]. Significant efforts were recently devoted to capture the behavior of these anomaly induced conductivities in WSMs [9-23].

The calculation of conductivity via the linear response formalism [39] inherently assumes a timescale τ_{ϕ} that can be interpreted as arising from interactions between the system and the external electric field that inelastically exchange energy at a rate $1/\tau_{\phi}$. The rate is assumed to be ideally zero, or in other words, τ_{ϕ} is assumed to be the largest of all relevant timescales. In the context of weakly disordered Weyl semimetals, when Landau quantization is relevant at high magnetic fields, chiral anomaly manifests itself by a positive contribution to the longitudinal magnetoconductance, i.e., $\mathbf{i} \propto$ $B(\mathbf{E} \cdot \mathbf{B})$, where **E** and **B** are the applied electric and magnetic fields. The current in this case is limited by the internode scattering time (τ_{inter}), which corresponds to a timescale at which quasiparticles scatter across the nodes and switch their chirality. Therefore, chiral charge is not conserved, but the global

charge remains conserved. For linear response formalism to work, τ_{inter} must be much less than τ_{ϕ} . Unfortunately, this approach breaks down if one considers intranode scattering as the *only* dominant scattering mechanism since, in this case, the chiral charge must remain conserved along with the global charge.

In the limit of weak magnetic field, Son and Spivak [10] highlighted the importance of internode-scattering-induced positive LMC in WSMs via the semiclassical Boltzmann approach. Despite this, a series of recent papers suggested that intranode scattering alone can give rise to positive longitudinal magnetoconductivity via an $\mathbf{E} \cdot \mathbf{B}$ force term incorporated in the semiclassical equations of motion [14–21]. It is therefore implied that positive LMC manifests in WSMs even in the limit when $\tau_{\text{inter}}/\tau_{\text{intra}} \rightarrow \infty$ (where τ_{intra} is the intravalley scattering time). Importantly, these works also made no distinction between the parameter regimes $\tau_{\rm intra} \ll \tau_{\phi} \ll \tau_{\rm inter}$ and $\tau_{\text{intra}} \ll \tau_{\text{inter}} \ll \tau_{\phi}$. The distinction between the two cases actually has drastic consequences, as chiral charge is conserved in the first, but the second indicates global charge conservation, which happens on a timescale larger than the intravalley timescale τ_{intra} , but smaller than τ_{ϕ} . The claim that intranode scattering alone can positively increase LMC, inherently assumes that $\tau_{\text{intra}} \ll \tau_{\phi} \ll \tau_{\text{inter}}$.

In this Letter, we show that the intranode scattering alone cannot yield positive LMC in WSMs, as this is inconsistent with chiral charge conservation. We begin by first showing that semiclassical calculations of LMC with a momentum-independent scattering time, as is assumed in the recent works [14-20], violate chiral charge conservation. Chiral charge conservation is shown to be consistent only with a momentum-dependent scattering rate, which, very importantly, yields a negative LMC. We therefore show that internode scattering is necessary to obtain positive LMC in Weyl semimetals, differently from the recent works. Even very weak internode scattering drives the system to show positive LMC, and only sufficiently strong intervalley scattering beyond a critical strength switches the sign to a negative LMC [21]. Chiral anomaly is therefore an internode phenomena in WSMs, even in the weak-B limit where the semiclassical formalism is valid, consistent with the Landau-level picture. Our results are fundamental for proper analysis of recent experimental results that claimed positive LMC to be a signature of chiral anomaly in the weak-field regime because we rule out the possibility of pure intravalley-scattering-induced positive LMC, which is not a true signature of chiral anomaly since it conserves chiral charge. Our results also have important consequences in the context of inhomogeneous WSMs (IWSMs), where we show that strain alone leads to a negative longitudinal magnetoconductance and contributes a planar Hall conductance which is of opposite sign to that of an external magnetic field. These results, which can be experimentally verified, are also in contrast to some other recent papers [40,41].

II. INCONSISTENCIES OF MOMENTUM-INDEPENDENT SCATTERING TIME

For a single isolated Weyl node $H_{\mathbf{k}} = \chi \hbar v_F \mathbf{k} \cdot \boldsymbol{\sigma}$, the steady-state Boltzmann equation takes the following form [42,43]:

$$e\mathcal{D}_{\mathbf{k}}^{\chi} \left(-\frac{\partial g_0}{\partial \epsilon_{\mathbf{k}}} \right) \left(\mathbf{v}_{\mathbf{k}}^{\chi} + \frac{e}{\hbar} \mathbf{B} \left(\Omega_{\mathbf{k}}^{\chi} \cdot \mathbf{v}_{\mathbf{k}}^{\chi} \right) \right) \cdot \mathbf{E} = \mathcal{I}_{\text{coll}} \{ g_{\mathbf{k}} \}, \quad (1)$$

where $\mathbf{v}_{\mathbf{k}}^{\chi}$ is the semiclassical band velocity, \mathbf{E} and \mathbf{B} are external electric and magnetic fields, respectively, $\Omega_{\mathbf{k}}^{\chi}$ is the Berry curvature [44], g_0 is the Fermi-Dirac distribution, $\epsilon_{\mathbf{k}}$ is the energy, and $\mathcal{D}_{\mathbf{k}}^{\chi} = (1 + e\mathbf{B} \cdot \Omega_{\mathbf{k}}^{\chi}/\hbar)^{-1}$. Within the relaxation-time approximation, the collision integral $\mathcal{I}_{\text{coll}}\{g_{\mathbf{k}}\}$ is simply

$$\mathcal{I}_{\text{coll}}\{g_{\mathbf{k}}\} = -\frac{\delta g_{\mathbf{k}}^{\chi}}{\tau_{\mathbf{k}}},\tag{2}$$

where $\delta g_{\bf k}^\chi$ is the deviation from the equilibrium. Particle conservation implies that

$$\sum_{\mathbf{k}} \delta g_{\mathbf{k}}^{\chi} = 0. \tag{3}$$

In the geometry when $\mathbf{E} \parallel \mathbf{B} \parallel \hat{z}$, the equation for particle conservation, Eq. (3), reduces to the following form [43]:

$$\int \tau^{\chi}(\theta) \left(v_z^{\chi} + \frac{e}{\hbar} B \left(\Omega_{\mathbf{k}}^{\chi} \cdot \mathbf{v}_{\mathbf{k}}^{\chi} \right) \right) \frac{k^3(\theta) \sin \theta}{|\mathbf{v}_{\mathbf{k}}^{\chi} \cdot \mathbf{k}|} d\theta = 0.$$
 (4)

Here all the quantities in the integrand are evaluated on the Fermi surface at zero temperature. A simplifying approach often employed is to assume that the scattering time is independent of momentum \mathbf{k} , i.e., $\tau^{\chi}(\theta) = \tau^{\chi}$ [14–20]. However, it can be easily verified from Eq. (4) that when $\tau^{\chi}(\theta)$ is independent of θ , the left-hand side (L.H.S.) of the equation does not reduce to zero. Even if we ignore the contribution due to the orbital magnetic moment, the integral above still turns out to be nonzero. For the case with a pair of Weyl nodes with zero

internode scattering, the chiral charge remains conserved and thus this result still remains valid. A momentum-independent scattering time is thus inconsistent with particle number conservation.

III. LMC FOR ZERO INTERNODE SCATTERING

When internode scattering is zero, it suffices to calculate the result for a single isolated Weyl node and the contribution from both the nodes can be summed over. Since we show that the momentum-independent relaxation time is not valid, we instead choose the collision integral in Eq. (1) to be

$$\mathcal{I}_{\text{coll}}\{g_{\mathbf{k}}\} = \sum_{\mathbf{k}'} \left(\Lambda_{\mathbf{k}}^{\chi} - \Lambda_{\mathbf{k}'}^{\chi}\right) W_{\mathbf{k}\mathbf{k}'}(-\partial g_0/\partial \epsilon_k) eE. \tag{5}$$

Here the scattering rate $W_{\mathbf{k}\mathbf{k}'}$ must not be taken to be independent of momenta, and without loss of generality, the unknown function $\Lambda^\chi_{\mathbf{k}}$ is assumed to be

$$\Lambda_{\mathbf{k}}^{\chi} = \left(f_{\mathbf{k}}^{\chi} - h_{\mathbf{k}}^{\chi} \right) \tau_{\mathbf{k}},\tag{6}$$

where $h_{\mathbf{k}}^{\chi} = \mathcal{D}_{\mathbf{k}}^{\chi} [v_z^{\chi} + e\hbar^{-1}B(\Omega_{\mathbf{k}}^{\chi} \cdot \mathbf{v}_{\mathbf{k}}^{\chi})]$, $\tau_{\mathbf{k}}^{-1} = \sum_{\mathbf{k'}} W_{\mathbf{k}\mathbf{k'}}$, and $f_{\mathbf{k}}^{\chi}$ is the unknown. The roles of the chemical potential and the orbital magnetic moment are incorporated by $(-\partial g_0/\partial \epsilon_k)$ and a B-dependent energy shift in the dispersion respectively. In the first Born approximation, and in the simplest case of point-like disorder, the scattering rate is evaluated to be

$$W_{\mathbf{k}\mathbf{k}'} = \frac{2\pi}{\hbar} |U|^2 \delta(\epsilon_{\mathbf{k}} - \epsilon_F)$$

$$\times [1 + \cos\theta \cos\theta' + \sin\theta \sin\theta' \cos(\phi - \phi')], \quad (7)$$

where U is the strength of the disorder in appropriate units. We emphasize that the explicit dependence on the direction of momenta, i.e., the polar and azimuthal angles, which comes from the chirality of the Weyl fermion wave function, survives even in the absence of momentum-dependent disorder strength U. The Boltzmann equation reduces to

$$f^{\chi}(\theta) = \int F^{\chi}(\theta')\tau(\theta)(1+\cos\theta\cos\theta')[f^{\chi}(\theta')-h^{\chi}(\theta')]d\theta',$$
(8)

where $F^{\chi}(\theta) = k^3(\theta)(\mathcal{D}_{\theta}^{\chi})^{-1}\sin\theta|\mathbf{v_k}\cdot\mathbf{k}|^{-1}$. Again, all the quantities in the integrand above are evaluated on the Fermi surface. To this end, incorporating particle conservation with the following ansatz solves the above Boltzmann transport equation:

$$\Lambda^{\chi}(\theta) = \tau(\theta)[a^{\chi} + b^{\chi}\cos\theta - h^{\chi}(\theta)], \tag{9}$$

Finally, the current due to the deviation in equilibrium is evaluated as

$$\mathbf{j}^{\chi} = -e \sum_{\mathbf{k}} \dot{\mathbf{r}}^{\chi} \left(\delta g_{\mathbf{k}}^{\chi} \right), \tag{10}$$

and the longitudinal conductivity $\sigma_{zz}(B)$ can be evaluated. We define $\delta\sigma_{zz}(B) = \sigma_{zz}(B) - \sigma_{zz}^0$, where σ_{zz}^0 is the zero-field conductivity. Figure 1(a) plots the evaluated LMC $\delta\sigma_{zz}(B)$ for an isolated Weyl node, which turns out to be always negative and independent of the chirality of the Weyl node. This result is in contrast to the recent papers concluding that intranode scattering alone can produce positive LMC in WSMs

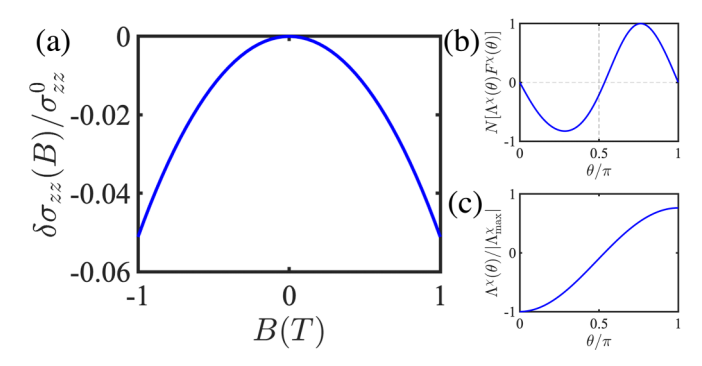


FIG. 1. (a) LMC for an isolated Weyl node is always negative due to chiral charge conservation. (b) $\Lambda^{\chi}(\theta)$ between 0 and π at B=1T. (c) The corresponding normalized deviation in the distribution function (proportional to δg_k^{χ}), which integrates to zero. Here $\chi=1$.

[14–21]. Figure 1(b) plots $\Lambda^{\chi}(\theta)$, while Fig. 1(c) plots the normalized distribution function. The distribution function directly reflects $\delta g_{\mathbf{k}}^{\chi}$, which integrates to zero, as expected from particle-number conservation. As a complementary approach, we also solve this problem using an ansatz-free numerical solution to the Boltzmann equation and reproduce the same findings [43]. We also approach this problem in the weak-B limit of Landau level formalism. In the presence of an external magnetic field (assumed to be parallel to the z-axis), the energy levels are quantized and the energy dispersion is given by $\epsilon_{n,\mathbf{k}_z} = v_F \operatorname{sign}(n) \sqrt{2\hbar |n|eB + (\hbar k_z)^2}$, where $n = \pm 1, \pm 2, \ldots$ (in addition to the chiral zeroth Landau level). The intraband conductivity is evaluated to be [43]

$$\sigma = \frac{\mathcal{C}}{2}(Bn_c - B),\tag{11}$$

where the prefactor C is a constant that depends on material parameters [43] and n_c is the number of filled Landau levels. We show that n_c scales linearly with B^{-1} [43] and therefore the magnetoconductivity due to intraband scattering for a single Weyl node is always negative.

IV. LMC WITH NONZERO INTERNODE SCATTERING

The collision integral takes the following form:

$$\mathcal{I}_{\text{coll}}\left\{f_{\mathbf{k}}^{\chi}\right\} = \sum_{\mathbf{k}'\chi'} \left(\Lambda_{\mathbf{k}}^{\chi} - \Lambda_{\mathbf{k}'}^{\chi'}\right) W_{\mathbf{k}\mathbf{k}'}^{\chi\chi'} (-\partial g_0/\partial \epsilon_k) eE, \quad (12)$$

where the scattering rate $W_{\mathbf{k}\mathbf{k}'}^{\chi\chi'}$ has internode as well as intranode scattering, which is evaluated to be

$$W_{\mathbf{k}\mathbf{k}'}^{\chi\chi'} = \frac{2\pi}{\hbar} |U^{\chi\chi'}|^2 \delta(\epsilon_{\mathbf{k}} - \epsilon_F)$$

$$\times \{1 + \chi\chi'[\cos\theta\cos\theta' + \sin\theta\sin\theta'\cos(\phi - \phi')]\},$$
(13)

where the disorder parameter $U^{\chi\chi'}$ allows us to tune the internode and intranode scattering strengths differently. Hereafter, we denote the ratio $|U^{\chi\neq\chi'}|^2/|U^{\chi=\chi'}|^2 \equiv \alpha$. The solution presented before is extended for the case of two nodes [43] with finite internode scattering. Figure 2(a) plots LMC for increasing intervalley scattering strength. We find that LMC for a pair of Weyl nodes of opposite chiralities becomes

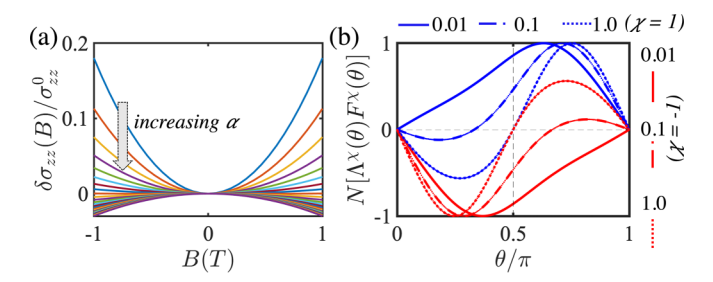


FIG. 2. (a) LMC for a pair of Weyl nodes of opposite chiralities becomes negative beyond a critical intervalley scattering strength α_c . Here α is increased from 0.1 to 1. (b) The normalized deviation in distribution functions at both the valleys for three different values of α .

negative beyond a critical intervalley scattering strength α_c , as was also observed in Refs [21,22]. This is attributed to an orbital magnetic moment that has opposite effect on the Fermi surfaces of both nodes [21] and renders them dissimilar in the presence of external magnetic field.

The striking observation here is that, even for weak internode scattering, LMC is positive, as opposed to the case of strictly zero internode scattering. The distribution function obtained here for the case of weak internode scattering is quite different from the one obtained in Fig. 1 for the case of zero internode scattering. In the later case the deviation of the distribution function must integrate out to zero at a single node, i.e., the chiral charge is conserved. This condition is relaxed in the presence of weak internode scattering and only the global charge needs to be conserved.

The Boltzmann transport equation gives the steady-state solution that is valid in the limit $t \gg \max\{\tau_{\text{inter}}, \tau_{\text{intra}}\}$. Hence, the particles are allowed to scatter and redistribute across both the nodes on a timescale much less than τ_{ϕ} . To highlight the role of τ_{ϕ} , we also incorporate it into the Boltzmann formalism [43]. We show that when $\tau_{\text{inter}} \gg \tau_{\phi}$, we are in an effective one-node regime and obtain negative LMC that are fully consistent with the results of a single-node obtained in the Letter. These observations summon very important points: (i) intranode scattering, by itself, does not yield positive LMC due to chiral charge conservation; (ii) finite internode scattering is fundamental for observing positive LMC in the semiclassical low-B limit; (iii) chiral anomaly induced positive LMC is therefore a pure internode phenomenon, reconciling the Boltzmann and the Landau-level picture; and (iv) sufficiently large internode scattering beyond a critical value α_c switches the sign of LMC from positive to negative. Correspondingly, $\tau_{\phi} \gg \tau_{\text{inter}} >$ $\tau_{\text{inter}}^{\text{c}}$ is necessary to observe positive LMC in experiments, where $\tau_{\text{inter}}^{\text{c}}$ is the critical intervalley scattering time below which LMC becomes negative. Figure 3 summarizes the conditions.

$\tau_{\phi} \gg \tau^{c}_{inter} > \tau_{inter} (-ve)$	$\tau_{\phi} \gg \tau_{\text{inter}} > \tau_{\text{inter}}^{\text{c}} (+\text{ve})$
$\tau_{\text{inter}} > \tau_{\phi} \gg \tau_{\text{intra}}$ (-ve)	$\tau_{\text{intra}} > \tau_{\phi} \gg \tau_{\text{inter}}$ (-ve)

FIG. 3. Conditions to observe positive or negative LMC.

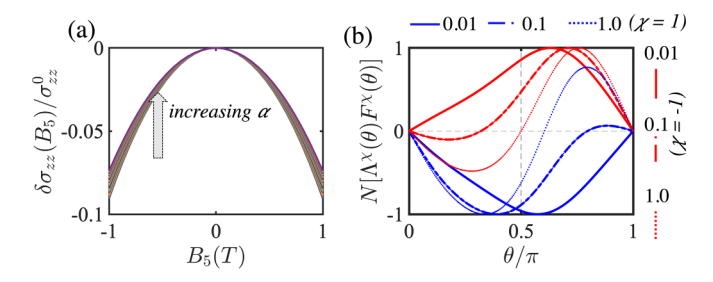


FIG. 4. (a) Strain-induced LMC for a pair of Weyl nodes of opposite chiralities is always negative. Here α is increased from 0.1 to 1. (b) The normalized deviation in distribution functions at both the valleys for three different values of α . B_5 field is chosen parallel to **E**.

V. INHOMOGENEOUS WSMS

We now show that our results have very important consequences in the characterization of Weyl systems with naturally occurring inhomogeneities. An axial magnetic field B₅ that couples to Weyl fermions of opposite chirality with an opposite sign can be realized by an inhomogeneous strain or magnetization profile in IWSMs [40,45,46]. Interestingly, it was pointed out that strain alone can result in a positive contribution to LMC even in the absence of external magnetic field $(\mathbf{B} = 0)$ [40]. In striking contrast, again, we discover that this result is incorrect and strain alone does not yield positive LMC, but rather decreases conductance, as plotted in Fig. 4(a). A detailed analysis of strain-induced LMC is presented in Ref. [43]. In the absence of strain, the switching of LMC from positive to negative is attributed to the effect of orbital magnetic moment, but here, ignoring that the OMM contribution does not affect our result qualitatively. This is because, unlike the previous case, strain-induced OMM affects both the nodes equally and thus the Fermi surfaces retain their similarity. We extend the formalism to the case of an inversion-asymmetric WSM. We choose a prototype model of a system with four Weyl nodes located at the points K = $(\pm \pi/2, 0, \pm \pi/2)$ in the Brillouin zone. The minimal model is given by

$$H = \sum_{n=1}^{4} \chi_n \hbar v_F \mathbf{k} \cdot \mathbf{\sigma},\tag{14}$$

where χ_n is the chirality of each Weyl node, and specifically, we choose $\chi_1 = -\chi_2 = \chi_3 = -\chi_4 = -1$ such that time-reversal symmetry is respected [see Fig. 5(a)]. We consider four possible internode scatterings as shown in the figure and scattering between diagonal nodes is neglected. Furthermore, we choose $\alpha^{12} = \alpha^{34}$ and $\alpha^{32} = \alpha^{14}$. The behavior of LMC without strain is plotted in Fig. 5(b). Sufficiently large internode scattering (α^{12} and/or α^{14}) yields negative LMC. In the presence of only strain-induced field B_5 , we never get a positive contribution to LMC as shown in Fig. 5(c).

VI. PLANAR HALL EFFECT IN IWSMs

To evaluate the planar Hall conductivity, the magnetic field is made noncollinear with the electric field direction. We rotate the magnetic field along the x-z plane that breaks the azimuthal symmetry [43]. Focusing on the strain-induced

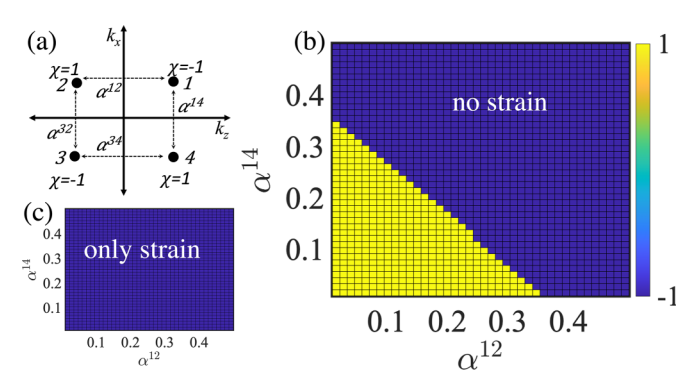


FIG. 5. (a) Minimal model of inversion asymmetric WSM with four nodes. Chirality of a node is indicated by χ and internode scattering from node i to j (and vice versa) is denoted by α^{ij} . The sign of LMC as a function of internode scattering without strain is plotted in (b) and with only strain in (c). Strain, alone does not increase LMC.

planar Hall effect, we find that, contrary to previous reports [41], the strain-induced contribution is not only opposite to that of the regular planar Hall effect, but also is different in magnitude. In Fig. 6 we explicitly show that, for the same orientation of the B and the B_5 field, the magnitude and the sign of planar Hall conductance are different from each other. Strain thus has a planar Hall conductance of opposite sign to that due to an external magnetic field.

VII. FINAL WORDS

Reconciling with the Landau-level picture, we show that chiral anomaly induced positive LMC is indeed an internode phenomenon, even in the weak-B semiclassical limit. Our results have remarkable implications in the context of Weyl semimetals, and are fundamental to a proper analysis of recent experiments. A positive LMC obtained in experiments in the weak-B limit must imply the manifestation of *true* chiral anomaly and excludes the possibility of intravalley scattering that conserves chiral charge.

ACKNOWLEDGMENTS

G. S. acknowledges support from SERB Grant No. SRG/2020/000134 and the IIT Mandi Startup Grant. S. T. acknowledges support from Grant No. NSF 2014157.

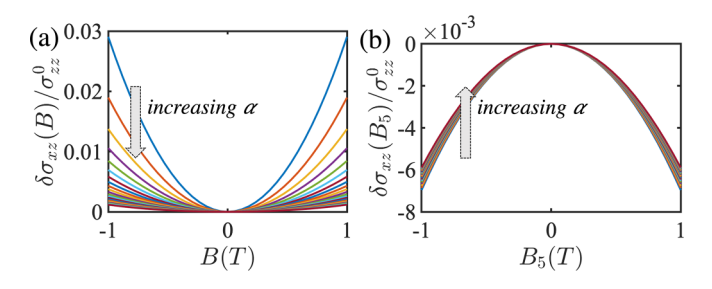


FIG. 6. (a) Planar Hall conductivity as a function of magnetic field in the absence of strain and (b) as a function of the axial magnetic field B_5 in the absence of external magnetic field. The angle of the magnetic field in (a) and axial field (b) are chosen to be the same.

- [1] S. L. Adler, Axial-vector vertex in spinor electrodynamics, Phys. Rev. 177, 2426 (1969).
- [2] J. S. Bell and R. Jackiw, A PCAC puzzle: $\pi^0 \rightarrow \gamma \gamma$ in the σ -model, Il Nuovo Cimento A (1965-1970) **60**, 47 (1969).
- [3] N. P. Armitage, E. J. Mele, and A. Vishwanath, Weyl and dirac semimetals in three-dimensional solids, Rev. Mod. Phys. 90, 015001 (2018).
- [4] G. E. Volovik, The Universe in a Helium Droplet (Oxford University Press on Demand, 2003), Vol. 117.
- [5] H. B. Nielsen and M. Ninomiya, No-Go theorum for regularizing chiral fermions, Technical Report No. RL-81-052, Science Research Council, 1981.
- [6] H. B. Nielsen and M. Ninomiya, The Adler-Bell-Jackiw anomaly and Weyl fermions in a crystal, Phys. Lett. B 130, 389 (1983).
- [7] X. Wan, A. M. Turner, A. Vishwanath, and S. Y. Savrasov, Topological semimetal and fermi-arc surface states in the electronic structure of pyrochlore iridates, Phys. Rev. B 83, 205101 (2011).
- [8] G. Xu, H. Weng, Z. Wang, X. Dai, and Z. Fang, Chern Semimetal and the Quantized Anomalous Hall Effect in HgCr₂Se₄, Phys. Rev. Lett. 107, 186806 (2011).
- [9] A. A. Zyuzin, S. Wu, and A. A. Burkov, Weyl semimetal with broken time reversal and inversion symmetries, Phys. Rev. B 85, 165110 (2012).
- [10] D. T. Son and B. Z. Spivak, Chiral anomaly and classical negative magnetoresistance of Weyl metals, Phys. Rev. B 88, 104412 (2013).
- [11] P. Goswami and S. Tewari, Axionic field theory of (3+1)dimensional Weyl semimetals, Phys. Rev. B 88, 245107 (2013).
- [12] P. Goswami, J. H. Pixley, and S. Das Sarma, Axial anomaly and longitudinal magnetoresistance of a generic three-dimensional metal, Phys. Rev. B 92, 075205 (2015).
- [13] S. Zhong, J. Orenstein, and J. E. Moore, Optical Gyrotropy from Axion Electrodynamics in Momentum Space, Phys. Rev. Lett. 115, 117403 (2015).
- [14] K.-S. Kim, H.-J. Kim, and M. Sasaki, Boltzmann equation approach to anomalous transport in a Weyl metal, Phys. Rev. B 89, 195137 (2014).
- [15] R. Lundgren, P. Laurell, and G. A. Fiete, Thermoelectric properties of Weyl and dirac semimetals, Phys. Rev. B 90, 165115 (2014).
- [16] A. Cortijo, Linear magnetochiral effect in Weyl semimetals, Phys. Rev. B 94, 241105(R) (2016).
- [17] G. Sharma, P. Goswami, and S. Tewari, Nernst and magnetothermal conductivity in a lattice model of Weyl fermions, Phys. Rev. B **93**, 035116 (2016).
- [18] V. A. Zyuzin, Magnetotransport of Weyl semimetals due to the chiral anomaly, Phys. Rev. B **95**, 245128 (2017).
- [19] K. Das and A. Agarwal, Berry curvature induced thermopower in type-i and type-ii Weyl semimetals, Phys. Rev. B 100, 085406 (2019).
- [20] A. Kundu, Z. B. Siu, H. Yang, and M. B. Jalil, Magnetotransport of Weyl semimetals with tilted dirac cones, New J. Phys. 22, 083081 (2020).
- [21] A. Knoll, C. Timm, and T. Meng, Negative longitudinal magnetoconductance at weak fields in Weyl semimetals, Phys. Rev. B **101**, 201402(R) (2020).

- [22] G. Sharma, S. Nandy, and S. Tewari, Sign of longitudinal magnetoconductivity and the planar Hall effect in Weyl semimetals, Phys. Rev. B **102**, 205107 (2020).
- [23] G. Bednik, K. S. Tikhonov, and S. V. Syzranov, Magnetotransport and internodal tunnelling in Weyl semimetals, Phys. Rev. Res. **2**, 023124 (2020).
- [24] L. P. He, X. C. Hong, J. K. Dong, J. Pan, Z. Zhang, J. Zhang, and S. Y. Li, Quantum Transport Evidence for the Three-Dimensional Dirac Semimetal Phase in Cd₃As₂, Phys. Rev. Lett. 113, 246402 (2014).
- [25] T. Liang, Q. Gibson, M. N. Ali, M. Liu, R. J. Cava, and N. P. Ong, Ultrahigh mobility and giant magnetoresistance in the dirac semimetal Cd₃As₂, Nat. Mater. 14, 280 (2015).
- [26] C.-L. Zhang, S.-Y. Xu, I. Belopolski, Z. Yuan, Z. Lin, B. Tong, G. Bian, N. Alidoust, C.-C. Lee, S.-M. Huang *et al.*, Signatures of the Adler–Bell–Jackiw chiral anomaly in a Weyl fermion semimetal, Nat. Commun. 7, 10735 (2016).
- [27] Q. Li, D. E. Kharzeev, C. Zhang, Y. Huang, I. Pletikosić, A. Fedorov, R. Zhong, J. Schneeloch, G. Gu, and T. Valla, Chiral magnetic effect in ZrTe₅, Nat. Phys. **12**, 550 (2016).
- [28] J. Xiong, S. K. Kushwaha, T. Liang, J. W. Krizan, M. Hirschberger, W. Wang, R. J. Cava, and N. P. Ong, Evidence for the chiral anomaly in the dirac semimetal Na₃Bi, Science 350, 413 (2015).
- [29] M. Hirschberger, S. Kushwaha, Z. Wang, Q. Gibson, S. Liang, C. A. Belvin, B. A. Bernevig, R. J. Cava, and N. P. Ong, The chiral anomaly and thermopower of Weyl fermions in the halfheusler GdPtBi, Nat. Mater. 15, 1161 (2016).
- [30] D. T. Son and N. Yamamoto, Berry Curvature, Triangle Anomalies, and the Chiral Magnetic Effect in Fermi Liquids, Phys. Rev. Lett. 109, 181602 (2012).
- [31] S. Nandy, G. Sharma, A. Taraphder, and S. Tewari, Chiral Anomaly as the Origin of the Planar Hall Effect in Weyl Semimetals, Phys. Rev. Lett. **119**, 176804 (2017).
- [32] P. Goswami, G. Sharma, and S. Tewari, Optical activity as a test for dynamic chiral magnetic effect of Weyl semimetals, Phys. Rev. B 92, 161110(R) (2015).
- [33] A. L. Levy, A. B. Sushkov, F. Liu, B. Shen, N. Ni, H. D. Drew, and G. S. Jenkins, Optical evidence of the chiral magnetic anomaly in the Weyl semimetal taas, Phys. Rev. B 101, 125102 (2020).
- [34] J.-M. Parent, R. Côté, and I. Garate, Magneto-optical kerr effect and signature of the chiral anomaly in a Weyl semimetal in magnetic field, Phys. Rev. B **102**, 245126 (2020).
- [35] Z. Song, J. Zhao, Z. Fang, and X. Dai, Detecting the chiral magnetic effect by lattice dynamics in Weyl semimetals, Phys. Rev. B **94**, 214306 (2016).
- [36] P. Rinkel, P. L. S. Lopes, and I. Garate, Signatures of the Chiral Anomaly in Phonon Dynamics, Phys. Rev. Lett. **119**, 107401 (2017).
- [37] X. Yuan, C. Zhang, Y. Zhang, Z. Yan, T. Lyu, M. Zhang, Z. Li, C. Song, M. Zhao, P. Leng *et al.*, The discovery of dynamic chiral anomaly in a Weyl semimetal NbAs, Nat. Commun. 11, 1 (2020).
- [38] B. Cheng, T. Schumann, S. Stemmer, and N. Armitage, Probing charge pumping and relaxation of the chiral anomaly in a dirac semimetal, Sci. Adv. 7, eabg0914 (2021).
- [39] G. D. Mahan, 9. Many-Particle Systems (Princeton University Press, Princeton, NJ, 2008).

- [40] A. G. Grushin, J. W. F. Venderbos, A. Vishwanath, and R. Ilan, Inhomogeneous Weyl and Dirac Semimetals: Transport in Axial Magnetic Fields and Fermi Arc Surface States from Pseudo-Landau Levels, Phys. Rev. X 6, 041046 (2016).
- [41] S. Ghosh, D. Sinha, S. Nandy, and A. Taraphder, Chirality-dependent planar Hall effect in inhomogeneous Weyl semimetals, Phys. Rev. B 102, 121105(R) (2020).
- [42] H. Bruus and K. Flensberg, *Many-Body Quantum Theory in Condensed Matter Physics: An Introduction* (Oxford University Press, New York, 2004).
- [43] See Supplemental Material at http://link.aps.org/supplemental/ 10.1103/PhysRevB.107.115161 for calculation details.
- [44] D. Xiao, M.-C. Chang, and Q. Niu, Berry phase effects on electronic properties, Rev. Mod. Phys. **82**, 1959 (2010).
- [45] A. Cortijo, Y. Ferreirós, K. Landsteiner, and M. A. H. Vozmediano, Elastic Gauge Fields in Weyl Semimetals, Phys. Rev. Lett. 115, 177202 (2015).
- [46] D. I. Pikulin, A. Chen, and M. Franz, Chiral Anomaly from Strain-Induced Gauge Fields in Dirac and Weyl Semimetals, Phys. Rev. X 6, 041021 (2016).